PERGAMON

Applied Thermal Engineering 21 (2001) 1407–1427

APPLIED THERMAL ENGINEERING

www.elsevier.com/locate/apthermeng

Integrated synthesis of process and heat exchanger networks: algorithmic approach

A.B. Nagy [a], R. Adonyi [a], L. Halasz [a], F. Friedler [a,*], L.T. Fan [b]

[a] *Department of Computer Science, University of Veszprem, Egyetem u. 10, Veszprem H-8200, Hungary*
[b] *Department of Chemical Engineering, Kansas State University, Manhattan, KS 66506, USA*

Received 10 January 2001; accepted 24 February 2001

Abstract

Methods exist for algorithmic process-network synthesis (PNS) as well as for heat-exchanger-network synthesis (HENS); nevertheless, such methods cannot be easily integrated for a variety of reasons. For instance, both PNS and HENS are complex problems; thus, their combination is naturally even more complex. Our previous effort to establish the combinatorial foundation of PNS has yielded a highly effective method involving the P-graph representation; the present approach to the integrated synthesis of process and heat-exchanger networks resorts mainly to hP-graphs adapted from the P-graphs in conjunction with the appropriate selection of inherent intervals of temperature range. This work focuses on the establishment of an appropriate technique for the integration of PNS and HENS. The resultant technique is largely based on combinatorics and combinatorial algorithms. The efficacy of the proposed approach is illustrated by solving an industrial problem.

Keywords: Process integration; Process synthesis; Heat-exchanger-network synthesis

1. Introduction

Algorithmic methods are available for process-network synthesis (PNS) generating flow sheets of processes as well as for heat-exchanger-network synthesis (HENS); however, these methods cannot be readily integrated for various reasons. For instance, the flow rates of streams are not specified a priori in PNS; in contrast, the flow rates and temperatures of hot and cold streams must be known as inputs in HENS. This difference can be attributed to the fact that the former is macroscopic in nature, while the latter is mesoscopic in nature; this gives rise to the characteristic

* Corresponding author. Tel.: +36-88-424-483; fax: +36-88-428-275.
E-mail address: friedler@dcs.vein.hu (F. Friedler).

1359-4311/01/$ - see front matter
PII: S1359-4311(01)00033-3

differences between them. Moreover, both PNS and HENS inevitably encounter combinatorial complexity; naturally, such complexity will magnify profoundly when they are integrated due to their interactions.

Heat integration in process synthesis is an extremely complex subject in the field of process system engineering; however, it is of utmost practical importance and of intense current interest. Attempts have been made to develop methods for such integration by resorting to pinch technology, simulation, heuristics and/or mixed integer programming based on the superstructure. Various degrees of success have been achieved for small or modest size processes, especially for mesoscopic systems such as separation and reactor sequences [1–5]. Nevertheless, much remains to be done to develop a highly efficient, rigorous algorithmic method for the integration that is readily implementable on a PC and applicable to a large-scale, realistic process.

The present paper aims at the development of an efficient technique for integrating PNS and HENS. The resultant technique is largely based on combinatorics and combinatorial algorithms. For simplicity, operating units, which are functional units of any process, such as reactors, separators and heat exchangers, are modelled here by linear functions. The proposed framework, however, is independent of the type of models of the operating units; therefore, it can be readily adapted for the synthesis involving operating units modelled by non-linear functions.

Our previous work to establish the foundation of PNS has given rise to a highly effective combinatorial method including the P-graph representation [6] and the accelerated branch-and-bound algorithm, i.e., algorithm ABB [7]. The current approach to the integrated synthesis of process and heat-exchanger networks resorts mainly to the hP-graphs adapted from the P-graphs and algorithm ABB in conjunction with the appropriate identification of the inherent intervals of temperature ranges of materials flowing through the process.

After a brief review of the combinatorial approach to process synthesis mentioned above, the proposed technique is elucidated with the aid of a hypothetical motivating example. This is followed by the application of the technique to a realistic industrial process, the toluene-hydroalkylation (HDA) process, to produce benzene [8].

2. Combinatorial approach to process synthesis: synopsis

In process synthesis, an unambiguous structural representation is required for formally analysing process structures. The process graph or P-graph, which is a directed bipartite graph, has been introduced for this purpose [6]. A brief description of it is given below.

Let M be a given finite non-empty set of objects, usually material species or materials that are to be transformed in the process under consideration. The transformation between two subsets of M occurs in an operating unit as illustrated in Fig. 1, where a circle represents a material, and a horizontal bar, an operating unit. It is necessary to link this operating unit to other operating units through the elements of these two subsets. P-graph (M, O) contains the interconnections among the operating units in set O (see Fig. 2).

The efficacy of P-graph representation in solving PNS problems has been amply demonstrated [7]. Nevertheless, it is incapable of tackling HENS problems by itself. Thus, P-graph representation need be modified by including additional features pertaining to heat exchange, as will be elaborated in connection with the motivating example.

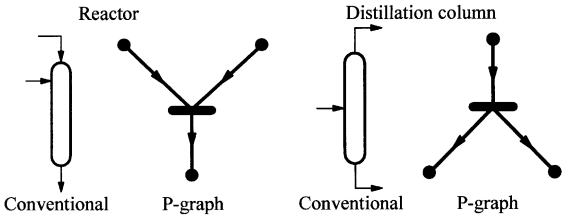

Fig. 1. Conventional and P-graph representations of a reactor and a distillation column.

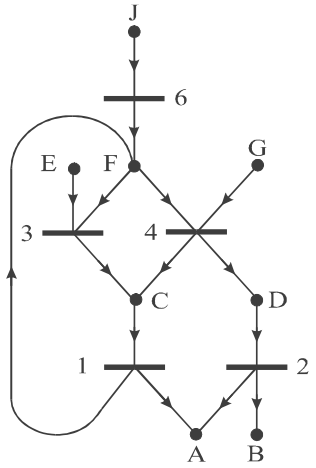

Fig. 2. P-graph representation of a network of operating units.

3. Motivating example

An optimal process is to be synthesised to produce material M_1 at a rate of 100 t/year by taking into account not only the cost of the process proper but also that of the subsidiary heat-exchanger network. Fig. 3 shows the maximal structure of the network of the process proper; the maximal structure is the superstructure with minimum complexity [9]. The operating units are represented by blocks; and their interconnections by lines with the directions of flows indicated by arrows. When the temperatures of the merging streams do not match, they must be modulated by heat-exchanging units, each comprising one or more heat exchangers and/or other heat-transfer devices, e.g., reboilers and condensers, in the process to be synthesised. It is unknown a priori which heat-exchanging units will be incorporated into the process. Thus, only the heating or cooling duty concomitant with each stream is noted in Fig. 3; it is marked by a horizontal bar. On each bar the heating is indicated by an arrow pointed upward from the left to the right; and the cooling, pointed downward from the left to the right. The maximal structure depicted in Fig. 3 naturally contains the potentially optimal structures. For example, the solution containing operating units 2, 5, and 7 is able to yield product M_1 from raw materials M_7, M_{10}, and M_{11}; therefore, it is one of the potentially optimal structures.

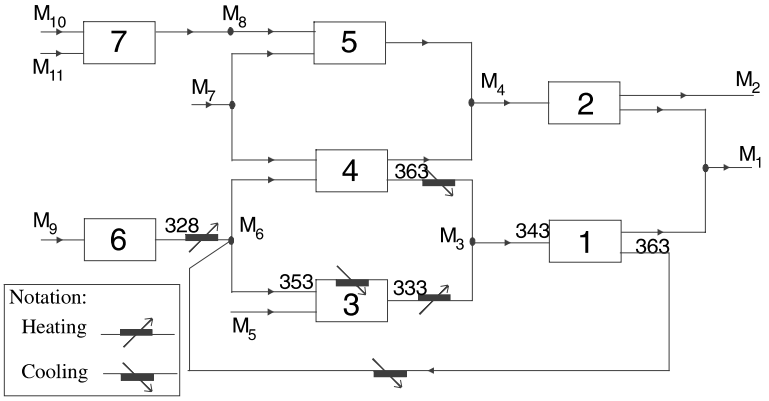

Fig. 3. Process flow sheet of the motivating example.

Suppose that the mathematical programming model and cost function of each operating unit are linear; then, an MILP model is appropriate for describing the network of the process proper in synthesis. Nevertheless, the subsidiary heat-exchanger network cannot be directly modelled from the maximal structure of the process proper; additional details need be provided for modelling. Parameters pertaining to the operating units are given in Table 1; and the data pertaining to the raw materials, in Table 2.

The heat production or consumption in an operating unit is determined by multiplying the coefficient of the latent heat source in Table 1 by the scaling factor relative to the unit with the prespecified capacity. For instance, a value of 20 in the table and a scaling factor of 2 imply that the heat production of operating unit 3 is 40 MJ. The flow rate of the input or output material of each operating unit for a prespecified capacity is given in the unit of t/h by the first number in the bracket following the name or symbol of materials. The second number after the comma is the temperature in the unit of K of the material if it is known.

The cost function of an operating unit comprises the investment and operating costs according to the following formula:

$$f(x) = \frac{Ia + Ibx}{\text{payout period}} + Oa + Obx \tag{1}$$

Table 1
Plausible operating units

Number	Latent heat temperature (K)	Latent heat source coefficient (MJ/h)	Input streams (t/h, K)	Output streams (t/h, K)
1	–	–	M_3(3,343)	M_1(2), M_6(1,363)
2	–	–	M_4(1.5)	M_1(1), M_2(0.5)
3	353	20	M_5(1), M_6(1,353)	M_3(2,333)
4	–	–	M_6(0.3), M_7(1.7)	M_3(1,363), M_4(1)
5	–	–	M_7(2), M_8(1)	M_4(3)
6	–	–	M_9(1)	M_6(1,328)
7	–	–	M_{10}(1.2), M_{11}(0.8)	M_8(2)

Table 2
Raw materials

Name	Price [USD/t]	Maximum flow [t/year]
M_5	140	Unlimited
M_7	200	Unlimited
M_9	250	Unlimited
M_{10}	50	Unlimited
M_{11}	70	Unlimited

where *Ia* and *Ib* are the constants pertaining to the investment cost; *Oa* and *Ob*, the constants pertaining to the operating cost; and x, the scaling factor of the operating unit (relative to the prespecified capacity). Moreover, the payout period is considered to be five years. The cost parameters of the operating units are listed in Table 3.

If the cooling and heating duties cannot be met within the structure, utilities must be used. Table 4 contains the parameters pertaining to such utilities.

The heat-transfer coefficients and area costs are regarded as identical for all heat exchangers. For simplicity, they are assumed to be 1.0 MJ/(h K m^2) and 5.0 USD/m^2, respectively.

3.1. hP-graph

The hP-graph is a special graph containing both operating and heat-exchanging units. Fig. 4 is the hP-graph representation of the flow sheet of the example illustrated in Fig. 3. The nodes for operating units are denoted by solid horizontal bars; and those for materials, by solid circles. The

Table 3
Cost parameters of the operating units

Operating unit	Investment cost (USD)		Operating cost (USD)	
	Ia	*Ib*	*Oa*	*Ob*
1	7,500	1,200	500	160
2	3,800	1,000	140	250
3	8,000	1,000	400	170
4	15,000	1,500	500	100
5	10,000	1,500	900	300
6	3,000	750	200	100
7	5,000	800	700	160

Table 4
Cost parameters of the utilities

Utility	Type	Temperature (K)	Cost (USD/MJ)
H_1	Hot	373.0	2.0
C_1	Cold	293.0	3.0

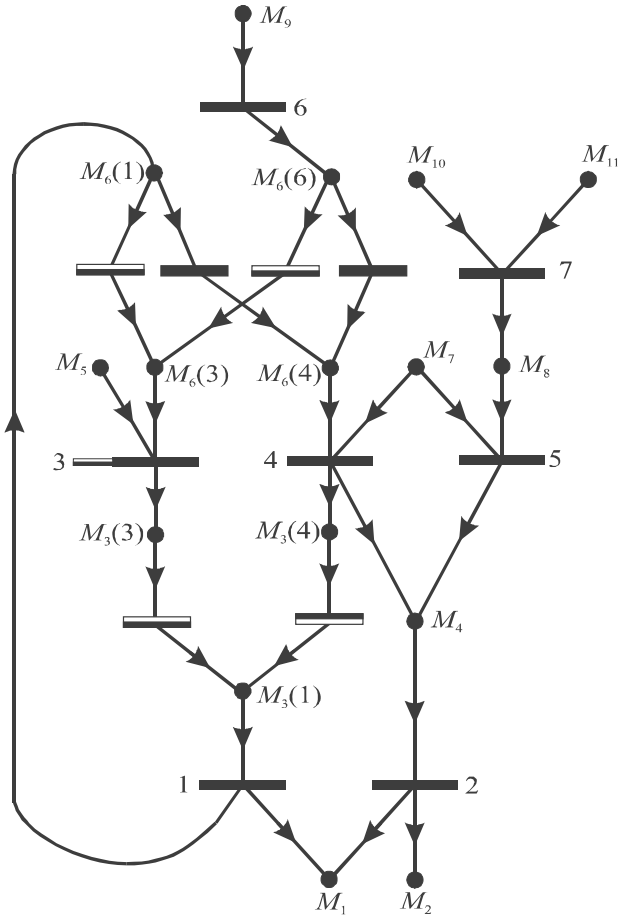

Fig. 4. hP-graph representing the integrated structure of the process and heat-exchanger networks of the motivating example.

node for a heat-exchanging unit for heating is indicated by a bar with a solid lower half; and that for cooling, by a bar with a solid upper half. When the content of any operating unit is heated or cooled by latent heat, the node for it is extended to the left by an appropriate heat-exchanging unit. For example, operating unit 3 is heated with hot latent heat. Suppose that part of a material stream feeding to an operating unit requires the temperature modulation, and the remaining part feeding to another operating unit does not. Then, the former is diverted through a heat-exchanging unit, and the latter, an undesignated operating unit. Each of the two streams of material M_6 is such a case.

3.2. Solution

The current example has been solved with algorithm ABB [7]. Fig. 5 illustrates the enumeration tree generated in implementing this algorithm.

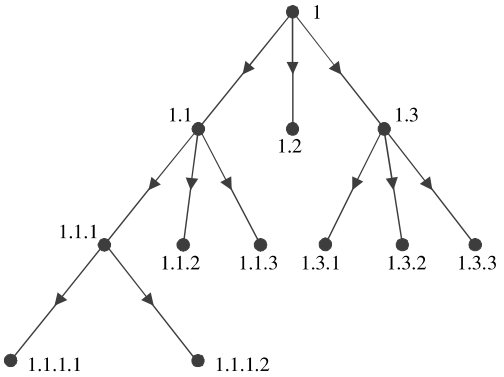

Fig. 5. Enumeration tree of the accelerated branch-and-bound algorithm for the motivating example (worst case).

Algorithm ABB determines if any of the operating units should be included in the optimal structure. Sets are assigned to the nodes of the tree to indicate the decisions made in the branching part of the algorithm. Set "Undecided" contains the operating units yet to be examined; set "Included" comprises those included in the partially generated structure; and set "Excluded" consists of those excluded from it. The leaves of the tree can be the candidate solutions of the problem. Table 5 lists the contents of the sets assigned to every node.

The first decision represented in the enumeration tree at node 1 is concerned with product M_1. It can be produced with operating unit 1, with operating unit 2, or with both of them. These possibilities are represented at nodes 1.1, 1.2 and 1.3, respectively. The next level of decisions involves the incoming materials of the newly included operating units. Such decisions are necessary as long as there are materials, which are not raw materials and not yet produced by any operating unit already included in the structure.

Each node of the search tree in Table 5 is associated with different models to be solved. For illustration, nodes 1 and 1.1.1.2 are elaborated in what follows.

Table 5
Partial problems examined

Node	Undecided operating units	Included operating units	Excluded operating units
1.	1,2,3,4,5,6,7	–	–
1.1	3,4,6	1	2,5,7
1.1.1	6	1,3	2,4,5,7
1.1.1.1	–	1,3	2,4,5,6,7
1.1.1.2	–	1,3,6	2,4,5,7
1.1.2	6	1,4	2,3,5,7
1.1.3	6	1,3,4	2,5,7
1.2	4,5,6,7	2	1,3
1.3	3,4,5,6,7	1,2	–
1.3.1	6	1,2,3,5,7	4
1.3.2	5,6,7	1,2,4	3
1.3.3	5,6,7	1,2,3,4	–

Node 1 (root): This is the first node; no decision is made at this node, and thus, set "Undecided" contains all the operating units. First, the proposed method determines the potential hot and cold streams. For this example, the method yields two potential hot streams and two potential cold streams, as summarised in Table 6. These streams are considered only as potential since their existence depends on the nature of the network of the process proper to be synthesised. Nevertheless, they need to be taken into account in a relaxed partial problem, e.g., that represented by node 1. Heating or cooling is necessary if the temperature of a material exiting from one operating unit is fed to another operating unit at a different temperature. For instance, operating unit 3 produces material M_3 at 333 K, which is fed to operating unit 1 at 343 K; thus, M_3 must be heated. One or more sources of latent heat can be assigned to a single operating unit. Table 7 lists the source of latent heat, i.e., stream LH_1 fed to operating unit 3.

Hot and cold streams can be indicated in the well-known cascade diagram as depicted in Fig. 6 where the temperatures of the cold streams are shifted upward by the approach temperature, which is regarded to be 10 K, to circumvent pinches. For example, cold stream S_3 of material M_3 varying from 333 to 343 K is rendered to range from 343 to 353 K. In the diagram, $I_1, I_2, \ldots,$ and I_5 signify the temperature intervals that are inherent in the temperatures of material streams passing through the process.

All hot and cold streams are divided into component substreams according to the inherent temperature intervals, $I_1, I_2, \ldots,$ and I_5; the hot component substreams are designated as FSH_1 through FSH_3, and the cold component substreams, as FSC_4 through FSC_7, as listed in Table 8.

A heat-exchanging unit or units can be established between any pair of a hot composite substream and a cold composite substream. Each of the composite substreams comprises one or more component substreams, which are adjacent, i.e., linked, to each other, as presented in Table 9.

A hot composite substream and a cold composite substream in Table 9 can be matched if the initial temperature of the former is greater than or equal to the final temperature of the latter. The hot and cold composite substreams can also be matched if the final temperature of the former is greater than or equal to the initial temperature of the latter. Accordingly, set $JSS(SSH_i)$ $(i = 1, 2, 3, 4)$ contains those composite substreams in Table 9 that can be matched with substream

Table 6
Potential hot and cold streams at node 1

Stream	Type	Material	Initial temperature (K)	Final temperature (K)
S_1	Hot	M_3	363	343
S_2	Hot	M_6	363	353
S_3	Cold	M_3	333	343
S_4	Cold	M_6	328	353

Table 7
Source of latent heat at node 1

Stream	Type	Operating unit	Temperature (K)
LH_1	Hot latent	3	353

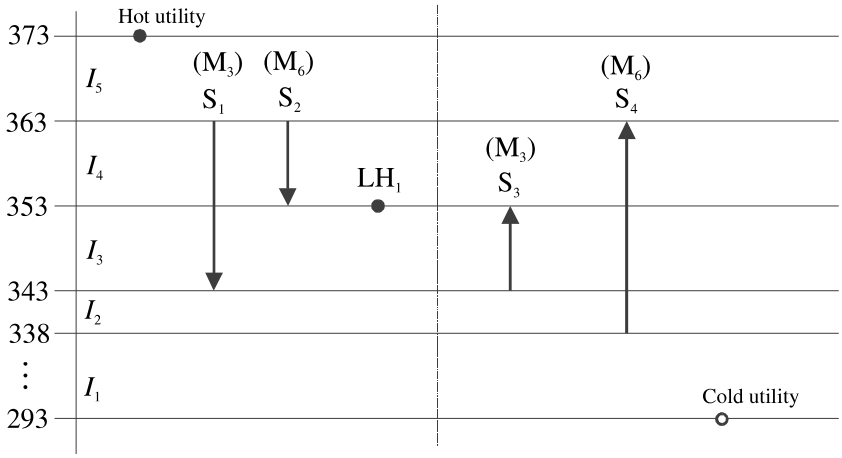

Fig. 6. Cascade diagram illustrating the inherent temperature intervals and hot and cold streams at node 1 of the motivating example.

Table 8
Hot and cold component substreams at node 1

Substream	Material	Type	Initial temperature (K)	Final temperature (K)
FSH_1	M_3	Hot	363	353
FSH_2	M_3	Hot	353	343
FSH_3	M_6	Hot	363	353
FSC_4	M_3	Cold	343	353
FSC_5	M_6	Cold	338	343
FSC_6	M_6	Cold	343	353
FSC_7	M_6	Cold	353	363

Table 9
Composite substreams at node 1

Substream	Interval	Material	Type	Initial temperature (K)	Final temperature (K)
SSH_1	I_3	M_3	Hot	353	343
SSH_2	I_4	M_3	Hot	363	353
SSH_3	I_3, I_4	M_3	Hot	363	343
SSH_4	I_4	M_6	Hot	363	353
SSC_5	I_3	M_3	Cold	343	353
SSC_6	I_2	M_6	Cold	338	343
SSC_7	I_3	M_6	Cold	343	353
SSC_8	I_4	M_6	Cold	353	363
SSC_9	I_2, I_3	M_6	Cold	338	353
SSC_{10}	I_3, I_4	M_6	Cold	343	363
SSC_{11}	I_2, I_3, I_4	M_6	Cold	338	363

SSH_i; naturally, if there is no appropriate substream to be matched, the set is empty. Listed below is all feasible $JSS(SSH_i)$'s.

$$JSS(SSH_1) = \{SSC_5, SSC_6, SSC_7, SSC_9\}$$
$$JSS(SSH_2) = \{SSC_5, SSC_6, SSC_7, SSC_8, SSC_9, SSC_{10}, SSC_{11}\}$$
$$JSS(SSH_3) = \{SSC_5, SSC_6, SSC_7, SSC_9, SSC_{10}, SSC_{11}\}$$
$$JSS(SSH_4) = \{SSC_5, SSC_6, SSC_7, SSC_8, SSC_9, SSC_{10}, SSC_{11}\}$$

The latent heat can be handled similarly to any composite stream. Set $JLS(LH_1)$, therefore, contains those composite substreams in Table 9 that can be matched to latent heat LH_1, i.e.,

$$JLS(LH_1) = \{SSC_5, SSC_6, SSC_7, SSC_9\}$$

The utilities can be matched with each component substream. Set $JSU(FSH_i)$ $(i = 1, 2, 3, 4)$ or set $JSU(FSC_i)$ $(i = 4, 5, \ldots, 11)$ contains those utilities that can potentially be matched with component substream FSH_i or FSC_i, respectively. For instance, for hot component substream FSH_i, a cold utility with a temperature of 293 K in this example is appropriate if the final temperature of this substream is greater than or equal to the temperature of the cold utility. All feasible $JSU(FSH_i)$'s and $JSU(FSC_i)$'s are given below.

$$JSU(FSH_1) = \{C_1\}, \quad JSU(FSH_2) = \{C_1\}, \quad JSU(FSH_3) = \{C_1\},$$
$$JSU(FSH_4) = \{C_1\}, \quad JSU(FSC_5) = \{H_1\}, \quad JSU(FSC_6) = \{H_1\}, \quad JSU(FSC_7) = \{H_1\}$$

where C_1 stands for cold utility 1, and H_1, hot utility 1. In general, cold utility i is indicated by C_i, and hot utility i, by H_i. The latent heats are handled similarly with respect to the utilities. Set $JLU(L_i)$ contains the utilities which can be appropriately matched to latent heat L_i; thus,

$$JLU(LH_1) = \{C_1\}$$

Even though the temperature of any substream is known, its enthalpy flow is not known for two reasons. First, the existence of a substream depends on the network structure of the process to be synthesised. Second, the flow rate of any substream, if it exists, depends on the operating conditions of the process. The specific heats of the materials which need to be heated or cooled are summarised in Table 10.

The rate of release or absorption of heat by a component substream inducing the change in its rate of enthalpy flow, QF_i $(i = 1, 2, \ldots, 7)$, is computed by multiplying the specific heat and flow rate of the material stream, and the corresponding inherent temperature interval; similarly, that by a source of latent heat inducing the change in its rate of enthalpy flow, QL_j $(j = 1)$, is computed by multiplying the coefficient of the latent heat source and the scaling factor of the pertinent operating unit. All QF_i's for the hot component substreams are taken to be positive; and those for

Table 10
Specific heats of materials

Material	Value
M_3	0.4
M_4	1.0
M_6	1.0

the cold component substreams, negative. Similarly, QL_i's for the hot latent heat sources are taken to be positive; those for the cold latent heat sources, negative.

The model relates QF_i's to the heat transfer between hot and cold composite substreams; it also relates QL_j's to the heat transfer between the sources of latent heat and composite streams. Thus, the pertinent variables of the model are the rates of heat transfer between the pairs of matched hot and cold composite substreams; these variables can be classified into different types according to the nature of matching. Each variable has two indices; the first indicates the hot substream, and the second, the cold substream. The variables can be identified with the aid of sets $JSS(SSH_i)$ $(i = 1, 2, 3, 4)$, and $JLS(LH_1)$. For instance, if set $JSS(SSH_i)$ contains substream SSC_j, then variable Q_{ij} expresses the rate of heat transfer from composite substream SSH_i to composite substream SSC_j. Table 11 contains the variables of the model related to these heat transfers.

Additional variables are defined for expressing the utility requirements for component substreams and sources of latent heats. Variable Q^*_{ik} indicates the rate of heat transfer between component substream FSH_i or FSC_i and cold utility C_k or hot utility H_k, respectively; similarly, QL^*_{ik} indicates the rate of heat transfer between hot latent heat source LH_i or cold latent heat source LC_i and cold utility C_k or hot utility H_k, respectively. Table 12 contains the variables of the model related to the utilities.

The significance of the change in the rate of enthalpy flow of component substream through the release and absorption of heat, which is transferred from composite substream i to composite substream j, with the rate, Q_{ij}, can be discerned in Fig. 7 in which stream is depicted with a rectangle. The length of the horizontal edge is proportional to the product of the specific heat and flow rate of the stream, while the vertical coordinate represents the temperature. The area of the rectangle represents the change in the rate of enthalpy flow of the stream. Let component substream FSH_k (rectangle EFGH) be specified by inherent temperature interval $[T_2, T_3]$; QF_k represented by the area of the rectangle denotes the change in the rate of enthalpy flow accompanying FSH_k which corresponds to QF_k. Also let SSH_i (rectangle ABCD) and SSC_j be composite substreams, between which heat is transferred; the temperature interval of the former be $[T_1, T_4]$; and

Table 11
Variables of the model at node 1

	SSC_5	SSC_6	SSC_7	SSC_8	SSC_9	SSC_{10}	SSC_{11}
SSH_1	$Q_{1\,5}$	$Q_{1\,6}$	$Q_{1\,7}$	–	$Q_{1\,9}$	–	–
SSH_2	$Q_{2\,5}$	$Q_{2\,6}$	$Q_{2\,7}$	$Q_{2\,8}$	$Q_{2\,9}$	$Q_{2\,10}$	$Q_{2\,11}$
SSH_3	$Q_{3\,5}$	$Q_{3\,6}$	$Q_{3\,7}$	–	$Q_{3\,9}$	$Q_{3\,10}$	$Q_{3\,11}$
SSH_4	$Q_{4\,5}$	$Q_{4\,6}$	$Q_{4\,7}$	$Q_{4\,8}$	$Q_{4\,9}$	$Q_{4\,10}$	$Q_{4\,11}$
LH_1	$QL_{1\,5}$	$QL_{1\,6}$	$QL_{1\,7}$	–	$QL_{1\,9}$	–	–

Table 12
Variables of the model pertaining to the utilities at node 1

	FSH_1	FSH_2	FSH_3	FSC_4	FSC_5	FSC_6	FSC_7	LH_1
C_1	$Q^*_{1\,1}$	$Q^*_{2\,1}$	$Q^*_{3\,1}$					$QL^*_{1\,1}$
H_1				$Q^*_{4\,1}$	$Q^*_{5\,1}$	$Q^*_{6\,1}$	$Q^*_{7\,1}$	

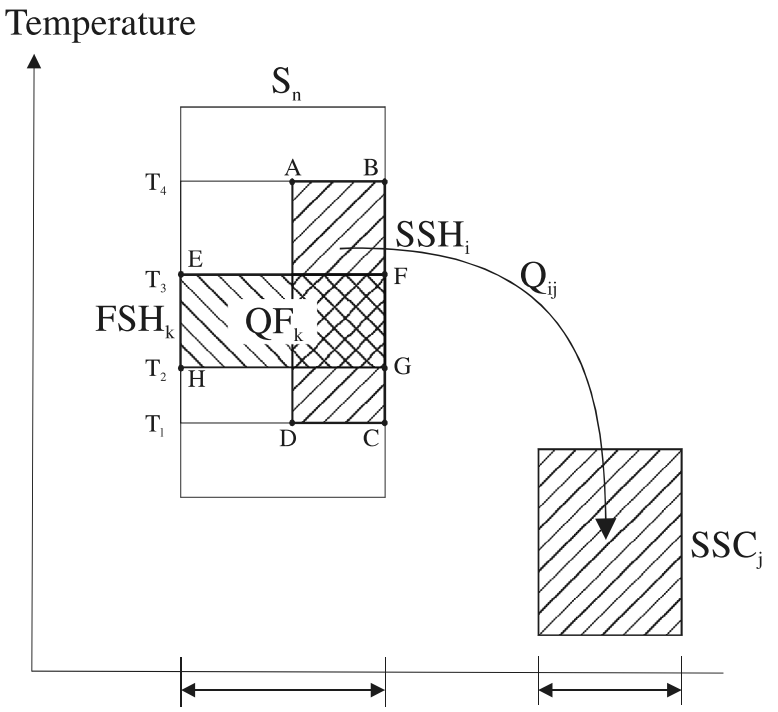

Fig. 7. Heat balance for a component substream of the motivating example: the horizontal coordinate represents the product of specific heat and flow rate of the respective stream, the significance of which manifests itself only in the magnitude of its interval.

the rate of heat transfer between them be Q_{ij}. Note that the areas of the rectangles for SSH_i (ABCD) and SSC_j are equal to Q_{ij}. The intersection of the rectangles for FSH_k (EFGH) and SSH_i (ABCD) represents the decrease in the rate of enthalpy flow accompanying FSH_k attributable to the heat transfer between SSH_i and SSC_j; it is equivalent to the portion of QF_k removed by this heat transfer, which can be calculated as

$$\frac{T_3 - T_2}{T_4 - T_1} Q_{ij} \tag{2}$$

The ratio of the two temperature intervals in the above expression is the coefficient of Q_{ij} in the heat balance equation for FSH_k.

Node 1 (root): This node involves seven component substreams and one source of latent heat. As an example, let us consider hot component substream FSH_2. The rate of heat release inducing the change in the rate of enthalpy flow accompanying it is denoted by QF_2. Every heat-exchanging unit which is taken into account in the heat balance equation for FSH_2 operates on the inherent temperature interval defining FSH_2, i.e., I_3. Every heat-exchanging unit, which transfers heat out of composite substream SSH_1 or SSH_3 must be considered. Naturally, both the temperature interval of SSH_1, i.e., I_3, and that of SSH_3, i.e., $I_3 \cup I_4$, contain the inherent temperature interval of FSH_2, i.e., I_3.

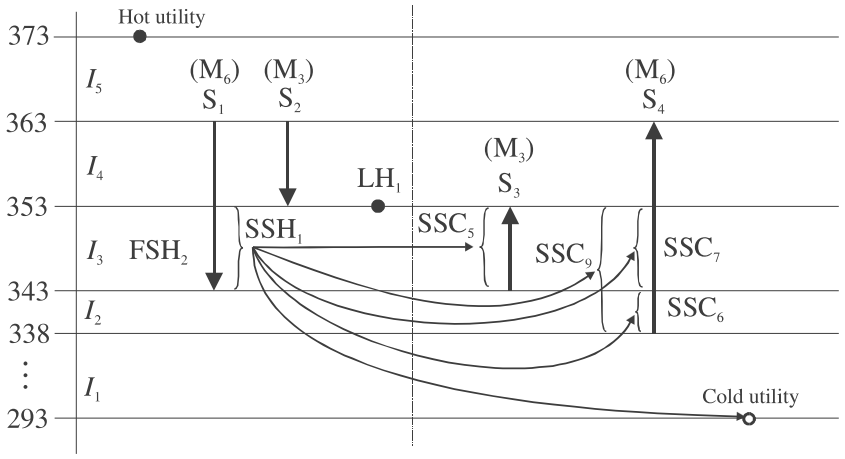

Fig. 8. Possible path of heat transfer from composite substream SSH_1 to composite substreams SSC_5, SSC_6, SSC_7, SSC_9, and cold utility at node 1 of the motivating example.

First, let us consider the possible heat transfer from hot composite substream SSH_1, whose temperature interval is I_3; four heat-exchanging units can transfer heat from this interval to appropriate cold subintervals as denoted by the arrows in Fig. 8; the heat exchanging units implementing this heat transfer correspond to the elements of set $JSS(SSH_1) = \{SSC_5, SSC_6, SSC_7, SSC_9\}$. Here, the temperature interval of composite substream SSH_1 and the inherent temperature interval of component substream FSH_2 are identical; it is I_3. The coefficient for these heat-exchanging units is computed by dividing the temperature interval of FSH_2 (353–343 K = 10 K) by that of SSH_1 (353 – 343 K = 10 K). The coefficient is one because the entire heat transferred is derived from component substream FSH_2.

Let us now consider the possible heat transfer from composite substream SSH_3, whose temperature interval is $I_3 \cup I_4$; six heat-exchanging units drain heat from interval as shown in Fig. 9.

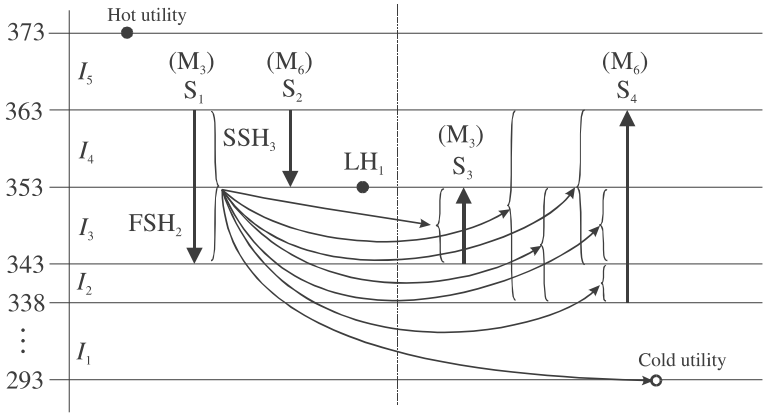

Fig. 9. Possible paths of heat transfer from composite substream SSH_3 to composite substreams SSC_5, SSC_6, SSC_7, SSC_9, SSC_{10}, SSC_{11}, and cold utility at node 1 of the motivating example.

Obviously, they can drain heat from FSH_2, whose temperature interval is I_3, and transfer it to the appropriate subintervals; these six heat exchanging units correspond to the elements of set $JSS(SSH_3) = \{SSC_5, SSC_6, SSC_7, SSC_9, SSC_{10}, SSC_{11}\}$. The coefficients related to the heat-exchanging units are computed by dividing the temperature interval of FSH_2 (353 − 343 K = 10 K) by that of SSH_3 (363 − 343 K = 20 K). The coefficient is 0.5 because only half of heat transferred is derived from the former.

There are no other possibilities to drain heat from inherent temperature interval I_3. This leads to the following heat balance equation for FSH_2.

$$0 = QF_2 - Q_{1\ 5} - 0.5Q_{3\ 5} - Q_{1\ 6} - 0.5Q_{3\ 6} - Q_{1\ 7} - 0.5Q_{3\ 7} - Q_{1\ 9} - 0.5Q_{3\ 9} - 0.5Q_{3\ 10} - 0.5Q_{3\ 11} - Q^*_{2\ 1}$$

The heat balance equations are also obtained for all other component substreams and the source of latent heat. The heat balance equations for all the component substreams and source of latent heat are listed below.

$$0 = QF_1 - Q_{2\ 5} - 0.5Q_{3\ 5} - Q_{2\ 6} - 0.5Q_{3\ 6} - Q_{2\ 7} - 0.5Q_{3\ 7} - Q_{2\ 8} - Q_{2\ 9} - 0.5Q_{3\ 9} - Q_{2\ 10} - 0.5Q_{3\ 10} - Q_{2\ 11} - 0.5Q_{3\ 11} - Q^*_{1\ 1}$$

$$0 = QF_2 - Q_{1\ 5} - 0.5Q_{3\ 5} - Q_{1\ 6} - 0.5Q_{3\ 6} - Q_{1\ 7} - 0.5Q_{3\ 7} - Q_{1\ 9} - 0.5Q_{3\ 9} - 0.5Q_{3\ 10} - 0.5Q_{3\ 11} - Q^*_{2\ 1}$$

$$0 = QF_3 - Q_{4\ 5} - Q_{4\ 6} - Q_{4\ 7} - Q_{4\ 8} - Q_{4\ 9} - Q_{4\ 10} - Q_{4\ 11} - Q^*_{3\ 1}$$

$$0 = QF_4 + Q_{1\ 5} + Q_{2\ 5} + Q_{3\ 5} + Q_{4\ 5} + QL_{1\ 5} + Q^*_{4\ 1}$$

$$0 = QF_5 + Q_{1\ 6} + Q_{2\ 6} + Q_{3\ 6} + Q_{4\ 6} + 0.3333Q_{1\ 9} + 0.3333Q_{2\ 9} + 0.3333Q_{3\ 9} + 0.3333Q_{4\ 9} + 0.2Q_{2\ 11} + 0.2Q_{3\ 11} + 0.2Q_{4\ 11} + QL_{1\ 6} + 0.3333QL_{1\ 9} + Q^*_{5\ 1}$$

$$0 = QF_6 + Q_{1\ 7} + Q_{2\ 7} + Q_{3\ 7} + Q_{4\ 7} + 0.6667Q_{1\ 9} + 0.6667Q_{2\ 9} + 0.6667Q_{3\ 9} + 0.6667Q_{4\ 9} + 0.5Q_{2\ 10} + 0.5Q_{3\ 10} + 0.5Q_{4\ 10} + 0.4Q_{2\ 11} + 0.4Q_{3\ 11} + 0.4Q_{4\ 11} + QL_{1\ 7} + 0.6667QL_{1\ 9} + Q^*_{6\ 1}$$

$$0 = QF_7 + Q_{2\ 8} + Q_{4\ 8} + 0.5Q_{2\ 10} + 0.5Q_{3\ 10} + 0.5Q_{4\ 10} + 0.4Q_{2\ 11} + 0.4Q_{3\ 11} + 0.4Q_{4\ 11} + Q^*_{7\ 1}$$

$$0 = QL_1 - QL_{1\ 5} - QL_{1\ 6} - QL_{1\ 7} - QL_{1\ 9} - QL^*_{1\ 1}$$

Table 13 summarises the coefficients of these balance equations.

The cost of heat exchange in the proposed mathematical model is deemed to be solely proportional to the heat transfer area between substreams i and j; thus,

$$c_{ij}Q_{ij} = a_{ij}\frac{1}{U_{ij}\,\mathrm{LMTD}_{ij}}Q_{ij} \tag{3}$$

Table 13
Coefficients of the heat balance equations at node 1

Variables	QF_1	QF_2	QF_3	QF_4	QF_5	QF_6	QF_7	QL_1
$Q_{1\,5}$		−1		1				
$Q_{2\,5}$	−1			1				
$Q_{3\,5}$	−1/2	−1/2		1				
$Q_{4\,5}$			−1	1				
$Q_{1\,6}$		−1			1			
$Q_{2\,6}$	−1				1			
$Q_{3\,6}$	−1/2	−1/2			1			
$Q_{4\,6}$			−1		1			
$Q_{1\,7}$		−1				1		
$Q_{2\,7}$	−1					1		
$Q_{3\,7}$	−1/2	−1/2				1		
$Q_{4\,7}$			−1			1		
$Q_{2\,8}$	−1						1	
$Q_{4\,8}$			−1				1	
$Q_{1\,9}$		−1			1/3	2/3		
$Q_{2\,9}$	−1				1/3	2/3		
$Q_{3\,9}$	−1/2	−1/2			1/3	2/3		
$Q_{4\,9}$			−1		1/3	2/3		
$Q_{2\,10}$	−1					1/2	1/2	
$Q_{3\,10}$	−1/2	−1/2				1/2	1/2	
$Q_{4\,10}$			−1			1/2	1/2	
$Q_{2\,11}$	−1				1/5	2/5	2/5	
$Q_{3\,11}$	−1/2	−1/2			1/5	2/5	2/5	
$Q_{4\,11}$			−1		1/5	2/5	2/5	
$QL_{1\,5}$				1				−1
$QL_{1\,6}$					1			−1
$QL_{1\,7}$						1		−1
$QL_{1\,9}$					1/3	2/3		−1
$Q^*_{1\,1}$	−1							
$Q^*_{2\,1}$		−1						
$Q^*_{3\,1}$			−1					
$Q^*_{4\,1}$				1				
$Q^*_{5\,1}$					1			
$Q^*_{6\,1}$						1		
$Q^*_{7\,1}$							1	
$QL^*_{1\,1}$								−1

where Q_{ij} is the rate of heat transfer; a_{ij}, the unit cost of heat-transfer area; U_{ij} the heat transfer coefficient; and $LMTD_{ij}$, the logarithmic mean temperature difference. Eq. (2) implies that the heat-transfer area computed on the basis of the logarithmic mean temperature difference, which is derived under the simplifying assumptions, suffices for the synthesis. These assumptions are that the heat-exchanging units are of the single-pass type and that one-dimensional, plug flow prevails in the streams. Table 14 contains the parameters of the cost function.

The prescribed mathematical model at node 1 is a linear programming (LP) model for the HEN part of the synthesis problem; adding the PNS part, consisting of the constraints and costs of the

Table 14
Parameters of the cost function at node 1

Variable	Coefficient c_{ij}	Variable	Coefficient c_{ij}
$Q_{1\,5}$	0.5000	$Q_{1\,9}$	0.4055
$Q_{2\,5}$	0.2500	$Q_{2\,9}$	0.2231
$Q_{3\,5}$	0.3465	$Q_{3\,9}$	0.2877
$Q_{4\,5}$	0.2500	$Q_{4\,9}$	0.2231
$Q_{1\,6}$	0.2876	$Q_{2\,10}$	0.3466
$Q_{2\,6}$	0.1823	$Q_{3\,10}$	0.5000
$Q_{3\,6}$	0.2310	$Q_{4\,10}$	0.3466
$Q_{4\,6}$	0.1823	$Q_{2\,11}$	0.3054
$Q_{1\,7}$	0.5000	$Q_{3\,11}$	0.4055
$Q_{2\,7}$	0.2500	$Q_{4\,11}$	0.3054
$Q_{3\,7}$	0.3466	$QL_{1\,5}$	0.3466
$Q_{4\,7}$	0.2500	$QL_{1\,6}$	0.2231
$Q_{2\,8}$	0.5000	$QL_{1\,7}$	0.3466
$Q_{4\,8}$	0.5000	$QL_{1\,9}$	0.3054

operating units, yields the solution which serves as the lower bound for the branch-and-bound algorithm.

Node 1.1.1.2 (leaf): At this node, operating units 1, 3 and 6 are included while all other operating units are excluded from the structure. Only those substreams linked to the former need be considered. Table 15 summarises the potential hot and cold streams, and Table 16 contains the source of the latent heat of partial problem 1.1.1.2.

Table 17 contains the hot and cold component substreams, which are generated by the inherent temperature intervals, $I_1, I_2, \ldots,$ and I_5, in Fig. 10. Table 18 lists the corresponding composite substreams.

Upon defining the heat-exchanging units and deriving the heat balance equations, the resultant LP model yields 51534 USD. Exploration of the entire enumeration tree indicates that the optimal solution of the motivating example is indeed generated at node 1.1.1.2 (leaf). This optimal solution contains only operating units 1, 3, and 6; the scaling factors for these operating units are 50, 75, and 25, respectively. The paths of heat transfer for this optimal solution are illustrated in Fig. 11.

4. Application

The toluene-hydrodealkylation (HDA) [8] comprises the reactor and separation systems, as shown in Fig. 12. The reactions involved are

$$\text{Toluene} + \text{H}_2 \rightarrow \text{Benzene} + \text{CH}_4$$

$$2\ \text{Benzene} \leftrightarrow \text{Diphenyl} + \text{H}_2$$

The streams of raw materials, toluene and hydrogen, are heated and combined with the recycled toluene and hydrogen streams before they are fed to the reactor. The product stream

Table 15
Potential hot and cold streams at node 1.1.1.2

Stream	Type	Material	Initial temperature (K)	Final temperature (K)
S_1	Hot	M_6	363	353
S_2	Cold	M_3	333	343
S_3	Cold	M_6	328	353

Table 16
Source of latent heat at node 1.1.1.2

Stream	Type	Operating unit	Temperature (K)
LH_1	Hot latent	3	353

Table 17
Hot and cold component substreams at node 1.1.1.2

Substream	Material	Type	Initial temperature (K)	Final temperature (K)
FSH_1	M_6	Hot	363	353
FSC_2	M_3	Cold	333	343
FSC_3	M_6	Cold	338	343
FSC_4	M_6	Cold	343	353
FSC_5	M_6	Cold	353	363

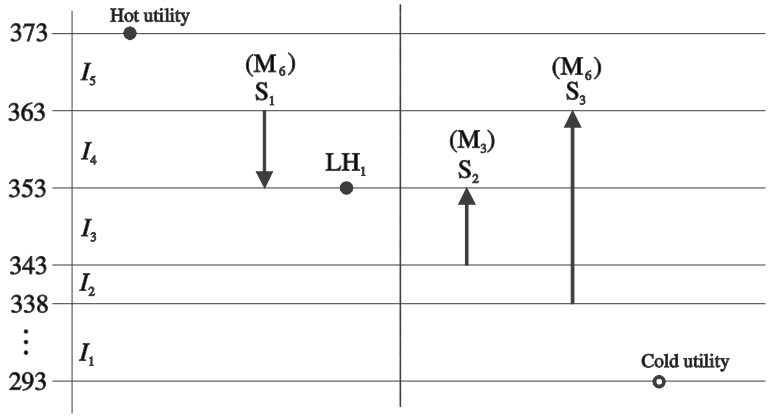

Fig. 10. Cascade diagram illustrating the inherent temperature intervals and hot and cold streams at node 1.1.1.2 of the motivating example.

leaving the reactor consists of hydrogen, methane, benzene, toluene, and the unwanted diphenyl. Most of the hydrogen and methane are separated by condensing aromatics and flashing away the light gases in a partial condenser.

Table 18
Composite substreams at node 1.1.1.2

Substream	Interval	Material	Type	Initial temperature (K)	Final temperature (K)
SSH_1	I_4	M_6	Hot	363	353
SSC_2	I_2	M_3	Cold	338	343
SSC_3	I_3	M_6	Cold	343	353
SSC_4	I_4	M_6	Cold	353	363
SSC_5	I_2, I_3	M_6	Cold	338	353
SSC_6	I_3, I_4	M_6	Cold	343	363
SSC_7	I_2, I_3, I_4	M_6	Cold	338	363

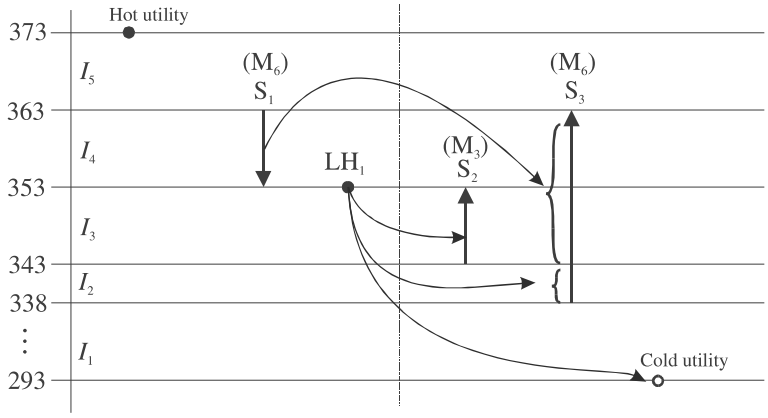

Fig. 11. Paths of heat transfer for the optimal solution of the motivating example.

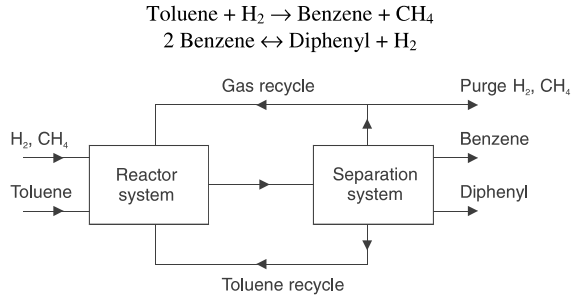

Fig. 12. Toluene-hydrodealkylation of the (HDA) process.

The hydrogen exiting from the flash is recycled, but the methane, which enters as an impurity in the hydrogen feed stream and is also produced by reaction, accumulates in the gas-recycle loop. Hence, a purge stream is required to remove both the feed and the methane generated from the process.

Not all hydrogen and methane can be separated from the aromatics in the flash drum; therefore, most of the remaining hydrogen and methane are removed by distillation to prevent them from contaminating the benzene product. Benzene is then recovered by distillation; finally, the recycled toluene is separated from the unwanted diphenyl also by distillation. The separation part of the system contains three simple and two complex separators.

In any process flow sheet, some streams must be heated, and others must be cooled. In the HDA process (Fig. 13), the fresh toluene feed, makeup hydrogen, recycle toluene, and recycle gas stream need be heated to the reaction temperature of 895 K. Also the reactor effluent stream need be cooled to the cooling water temperature to accomplish the phase split. There are also heating and cooling loads on the distillation-column reboilers and condensers, respectively.

The system consists of four cold and four hot streams, a reactor heat effect, and five hot and five cold latent heat sources for the corresponding separators. The number of hot component substreams is 14, and that of the cold component substreams is 48. This results in $48 + 14 = 62$ linear

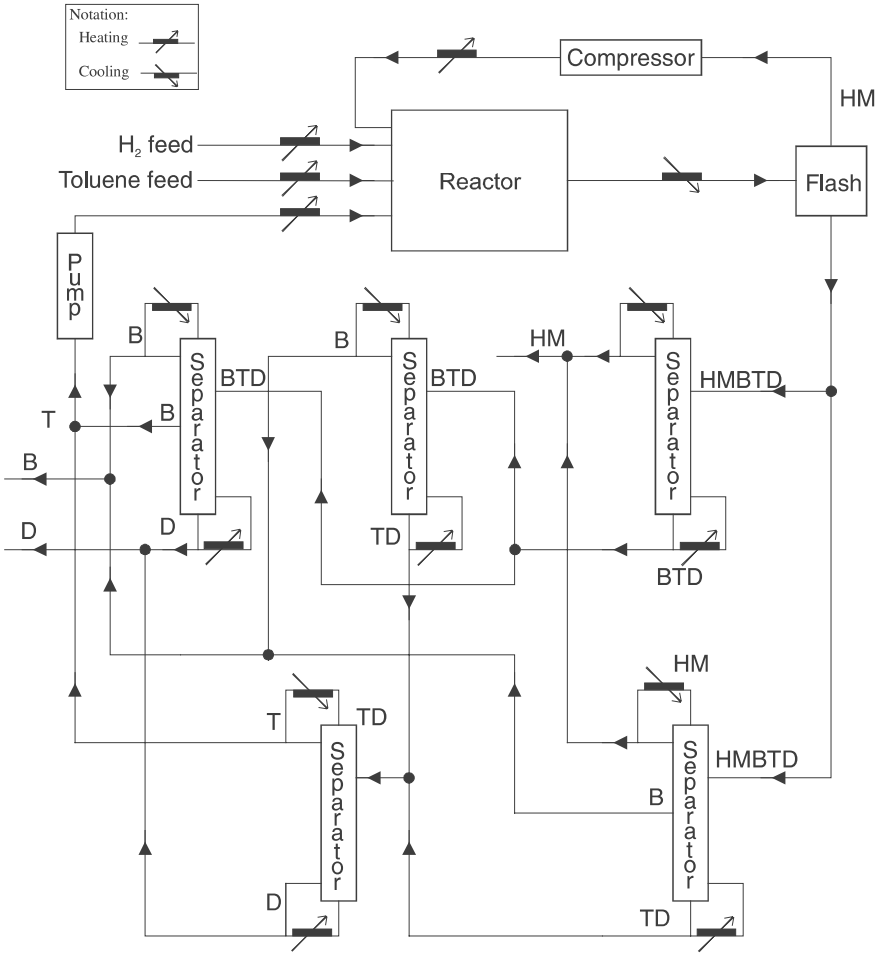

Fig. 13. Flow sheet of the HDA process.

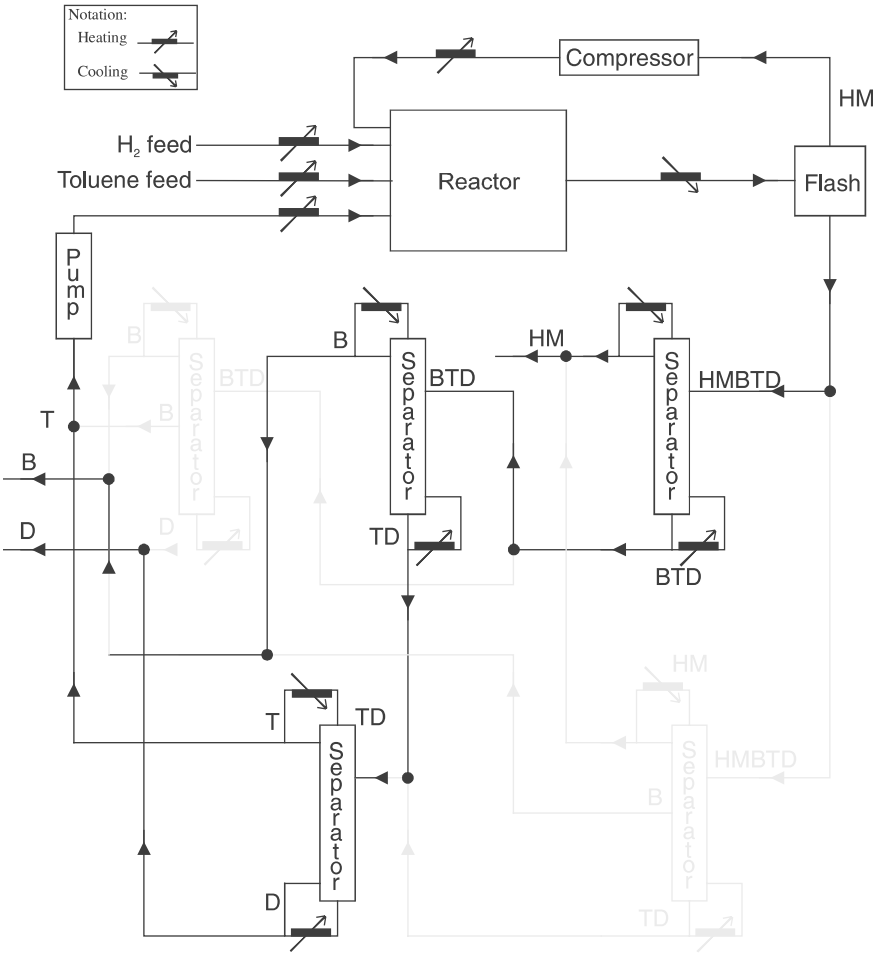

Fig. 14. Optimal solution of the HDA problem.

constraints belonging to the HEN model. There are 105 cold composite substreams and 333 hot composite substreams, thereby yielding 10,227 potential heat-exchanging units. The number of inherent temperature intervals is 18.

The current procedure yields the optimal solution within 96.07 s on a PC (Celeron 400 MHz). The resultant optimal solution is illustrated in Fig. 14, which contains seven operating units and 18 heat-exchanging units.

5. Concluding remarks

A combinatorial method of PNS has been effectively combined with that of HENS for the integrated synthesis of process and heat-exchanger networks. The application to the synthesis of a realistic process has proved that the combined method's efficacy is indeed remarkable.

Acknowledgements

This work was partially performed during the tenure of one of the authors (FF) as a holder of the Science Fellowship at the Department of Process Integration, UMIST, Manchester, UK under the auspices of The British Council.

References

[1] M.A. Duran, I.E. Grossmann, Simultaneous optimization and heat integration of chemical processes, AIChE J. 32 (1986) 123–138.
[2] I.E. Grossmann, H. Yeomans, Z. Kravanja, A rigorous disjunctive optimisation model for simultaneous flow sheet optimisation and heat integration, Comput. Chem. Engng. 22 (1998) S157–S164.
[3] Y.D. Lang, L.T. Biegler, I.E. Grossmann, Simultaneous optimisation and heat integration with process simulators, Comput. Chem. Engng. 12 (1988) 311–327.
[4] L.T. Biegler, I.E. Grossmann, A.W. Westerberg, Systematic Methods of Chemical Process Design, Prentice Hall PTR, New Jersey, 1997, pp. 567–617.
[5] R. Smith, Chemical Process Design, McGraw-Hill, New York, 1994.
[6] F. Friedler, K. Tarjan, Y.W. Huang, L.T. Fan, Graph-theoretical approach to process synthesis: axioms and theorems, Chem. Engng. Sci. 47 (1992) 1973–1988.
[7] F. Friedler, J.B. Varga, E. Fehér, L.T. Fan, Combinatorial accelerated branch-and-bound method for solving the MIP model of process network synthesis, in: C.A. Floudas, P.M. Pardalos (Eds.), Nonconvex Optimization and its Applications, Kluwer Academic Publishers, Norwell, MA, USA, 1996, pp. 609–626.
[8] J.M. Douglas, Conceptual Design of Chemical Processes, McGraw-Hill, New York, 1988.
[9] F. Friedler, K. Tarjan, Y.W. Huang, L.T. Fan, Graph-theoretical approach to process synthesis: polynomial algorithm for maximal structure generation, Comput. Chem. Engng. 17 (1993) 929–942.